RESEARCH ARTICLE

# STM32-based self-powered biosensor network for tunnel environmental air quality monitoring using piezoelectric energy harvesting

Guangliang Cui[1], Xuejun Di[2, *], Hai Yishar Smair[3], Yespola Ti Yemai[4], Junyi Liu[2]

[1]Xinjiang Uygur Autonomous Region Transportation Construction Affairs Center, Urumqi, Xinjiang, China. [2]China First Highway Engineering Co., LTD, Beijing, China. [3]Maintenance Department of Changji Highway Development Center, Urumqi, Xinjiang, China. [4]Technology Department of the Xinjiang Uygur Autonomous Region Railway and Civil Aviation Development Center, Urumqi, Xinjiang, China.

**Received:** April 26, 2026; **accepted:** May 26, 2026.

**With the rapid expansion of highway tunnel networks, accumulated vehicle exhaust pollutants such as $PM_{2.5}$, NOx, and CO pose increasing risks to traffic safety and passenger health, making real-time monitoring of tunnel ambient air quality essential. Traditional wired monitoring systems suffer from cumbersome wiring, high maintenance costs, and susceptibility to power outages, while battery-powered wireless systems are constrained by short battery life. To overcome these limitations, this study developed a self-powered wireless tunnel air quality monitoring system that harvested vibration energy generated by passing vehicles within the tunnel. An STM32 microcontroller was integrated with piezoelectric sensors to construct the system hardware, encompassing the energy harvesting, power management, data acquisition and processing, and wireless communication circuits, and a simulated tunnel environment test platform was established for performance evaluation. The system achieved a peak output power of approximately 1.8 mW at a vibration frequency of 40 Hz, accurately measured temperature, humidity, $PM_{2.5}$, and harmful gas concentrations with errors within acceptable limits compared with reference equipment and operated stably during a 72-hour continuous test with energy harvesting and consumption maintained in dynamic balance. The proposed system efficiently harvested vibration energy and reliably monitored tunnel ambient air quality, offering a maintenance-free solution that safeguarded tunnel safety operations and passenger health and was expected to become a preferred approach for future tunnel ambient air monitoring applications.**

**Keywords:** tunnel environment; air quality; monitoring; energy harvesting; STM32 microcontroller; piezoelectric sensor; wireless system.

***Corresponding author:** Xuejun Di, China First Highway Engineering Co., LTD, Beijing 100010, China. Email: yaxmzo113@163.com.

## Introduction

With the rapid development of national highway tunnel construction, the number and total length of tunnels continue to increase. However, issues regarding indoor air quality within tunnels have become increasingly prominent, posing a serious threat to traffic safety and passenger health [1]. Pollutants such as particulate matter ($PM_{2.5}$), nitrogen oxides (NOx), and carbon monoxide (CO) from vehicle exhaust accumulate inside tunnels, resulting in traffic accidents caused by poor indoor air quality accounting for over 15% of all incidents [2]. Traditional wired monitoring systems suffer from drawbacks such as complex wiring, high maintenance costs, and susceptibility to power outages. Meanwhile, wireless monitoring systems rely on battery power, requiring frequent battery replacements, which not only increases labor and material costs but may also cause environmental pollution [3]. Energy harvesting technology offers a new approach to tunnel ambient air monitoring. By using piezoelectric sensors to convert the mechanical energy from vehicle vibrations into electrical energy, it enables self-powered wireless monitoring systems [4], which not only eliminates the need for battery replacement and reduces maintenance costs but also enhances system operational stability, providing an innovative solution for tunnel ambient air monitoring [5, 6].

Tunnel environmental air monitoring and energy harvesting technology are currently hot research areas, and they are of great significance for improving tunnel safety and sustainability. In terms of tunnel ambient air monitoring, many studies have focused on developing high-performance sensor networks to achieve real-time, accurate ambient air quality monitoring [7]. Jegadeesan *et al*. proposed a wireless sensor network-based tunnel ambient air quality monitoring system capable of monitoring various pollutants such as CO, nitrogen dioxide ($NO_2$), and $PM_{2.5}$ with good sensitivity and stability [8]. Additionally, Shaker *et al*. utilized machine learning algorithms to analyze and predict monitoring data, thereby enhancing the intelligence of the monitoring system [9]. Regarding energy harvesting technologies, researchers have explored various energy sources including vibration, solar energy, and temperature differences to achieve self-powered monitoring systems [10–12]. Particularly in the field of vibration energy harvesting, piezoelectric sensors have been extensively studied due to their high efficiency and stability. Chen *et al*. described a vibration energy harvesting device based on piezoelectric ceramics capable of effective energy harvesting across a wide frequency range [13]. Meanwhile, Mukogawa *et al*. combined multiple energy harvesting technologies to improve the system's energy output and stability [14]. Although these studies have made some progress, several challenges remain. There is a lack of broadband piezoelectric energy harvesting solutions suitable for tunnel environments [15]. Energy harvesting efficiency is a concern, making it difficult to meet the power consumption requirements of monitoring systems [16]. System integration is low with poor coordination among energy harvesting, sensing, and communication modules [17].

This research proposed an energy harvesting solution for a wireless tunnel ambient air monitoring system based on an STM32 microcontroller and piezoelectric sensors. A high-efficiency piezoelectric energy harvesting circuit was designed by adopting synchronous charge extraction technology to improve energy conversion efficiency, allowing the system to effectively utilize vehicle vibration energy within the tunnel and achieve self-powering. The system hardware architecture was further optimized by integrating temperature, humidity, $PM_{2.5}$, and harmful gas sensors to enable multi-parameter environmental air monitoring, and the accuracy and flexibility of data acquisition were enhanced through a dedicated interface circuit and channel expansion methods. In addition, a low-power Bluetooth module was adopted to enable the remote transmission of monitoring data, ensuring stable data transmission and strong resistance to interference. The results of this research proposed a novel system for energy harvesting efficiency, data acquisition accuracy, and stability and provided a maintenance-free wireless solution for tunnel ambient air monitoring.

## Materials and methods

### Piezoelectric energy harvesting circuit design

The design of the piezoelectric energy harvesting circuit primarily consisted of a piezoelectric element interface circuit and a signal conditioning and conversion circuit. These two components worked in tandem to ensure that weak piezoelectric signals were effectively converted into usable electrical energy. The design of interface circuits for piezoelectric elements focused on optimizing energy conversion efficiency. The electrical energy generated by piezoelectric sensors was typically weak and unstable, so an efficient interface circuit was required to maximize energy extraction. Synchronous charge extraction (SCE) technology was employed in this study, which effectively improved energy conversion efficiency by switching the circuit in sync with the resonant frequency of the piezoelectric sensor [18]. This technology ensured that as much electric charge as possible was extracted during every vibration cycle of the piezoelectric sensor. In the circuit design, the parameters of the interface circuit were calculated as follows.

$$P_{out} = \frac{V_{pzt}^2}{4R_{on}} \quad (1)$$

where $P_{out}$ was the output power. $V_{pzt}$ was the open-circuit voltage of the piezoelectric sensor. $R_{on}$ was the on-resistance of the metal-oxide-semiconductor field-effect transistor (MOSFET). The task of the signal conditioning and conversion circuit was to amplify, filter, and convert the weak signals output by the piezoelectric elements into electrical energy suitable for storage and use [19]. The signal was amplified by a low-noise operational amplifier to enhance its strength followed by passing through a bandpass filter to remove unwanted noise frequencies and ensure signal purity. To further improve energy availability, this study designed a rectification circuit in this part to convert the alternating current (AC) signal into a direct current (DC) signal. The DC signal then passed through a DC-DC converter to regulate it to the voltage level required by the system. The design of the entire signal conditioning and conversion circuit fully considered efficiency and stability, ensuring maximum utilization of energy.

**Power management circuit design**

The power management circuit was designed to ensure the effective storage and rational distribution of energy to meet the power supply requirements of various system components. The charging and energy storage circuit was responsible for storing the harvested energy to provide stable power support for the system. This study selected supercapacitors as energy storage components due to their high-power density and rapid charging and discharging capabilities. The energy storage for supercapacitors was calculated as follows.

$$E = \frac{1}{2}CV^2 \quad (2)$$

where *E* was stored energy. *C* was the capacitance. *V* was the voltage. To achieve efficient charging control, this study designed an intelligent charging circuit based on a comparator, which automatically adjusted the charging current according to the voltage level of the supercapacitor to prevent overcharging and over-discharging. The voltage regulation and power distribution circuit ensured that all parts of the system received a stable and appropriate voltage. This study employed a high-efficiency buck DC-DC converter to convert the high voltage of the supercapacitor into the low voltage required by the system. By adjusting the duty cycle of the DC-DC converter, the output voltage could be precisely controlled to meet the power supply requirements of different modules. The STM32 microcontroller (STMicroelectronics, Geneva, Switzerland) and its peripheral logic operated at 3.3 V with a typical current draw of about 30 mA in active mode. The analog front-end and signal-conditioning circuitry were powered at 3.3 V at approximately 10 mA. The air-quality sensor module for temperature, humidity, $PM_{2.5}$, and harmful gas sensors was supplied with 5 V at about 50 mA. The low-power Bluetooth module operated at 3.3 V and about 15 mA in transmission mode. These voltage and current levels were used to size the buck DC-DC stages and to verify that the harvested energy could sustain steady-state operation.

**Data acquisition circuit design**

**(1) Environmental air quality sensor interfaces**

When designing the data acquisition circuit, special attention should be paid to efficiently acquiring key ambient air quality parameters such as temperature, humidity, $PM_{2.5}$, and harmful gases. Through an in-depth analysis of these sensors' characteristics, this study developed an interface circuit capable of accurately collecting the relevant data. For temperature and humidity sensors, this study adopted a design scheme combining a capacitive humidity sensing element with a thermistor and used a simple voltage-to-current conversion circuit to convert the sensor's output signal into a voltage signal suitable for an analog-to-digital converter (ADC) acquisition as follows.

$$V_{out} = K \cdot \left( R_h + R_t \right) \quad (3)$$

where $V_{out}$ was the output voltage. $K$ was the conversion coefficient. $R_h$ and $R_t$ were the resistance values of the humidity and temperature sensors, respectively. In the design of the $PM_{2.5}$ sensor interface, the principle of scattered light measurement was employed, and a low-noise signal amplification circuit was incorporated to amplify the sensor's weak output signal. The amplified signal was digitized using a 16-bit ADC to ensure high-resolution and accurate data. The harmful gas sensor employed an electrochemical detection principle. To accommodate the detection requirements of different gases, this research designed a multi-channel sensor interface circuit capable of simultaneously supporting the detection of multiple harmful gases. This circuit switched between different gas sensor signals *via* a multiplexer and acquired data through a high-precision ADC. The four sensor interface circuits adopted in this study covered complementary measurement principles and signal-conditioning needs. The temperature/humidity interface used a capacitive-plus-thermistor configuration with a voltage-to-current conversion stage and a 12-bit ADC channel for low-bandwidth (~ 1 Hz) measurements. The $PM_{2.5}$ interface employed the scattered-light principle combined with a low-noise amplifier and a 16-bit ADC to resolve weak optical signals. The harmful-gas interface used electrochemical sensing with a multiplexed high-precision (16-bit) ADC channel to support several target gases on a single front end. Together, they provided a balanced trade-off between resolution, channel count, and power consumption suited to a self-powered monitoring node.

**(2) Data acquisition channel expansion**

To meet the system's requirements for multi-parameter monitoring, this study designed a flexible method for expanding data acquisition channels. By employing analog switch and multiplexer technologies, the system's data acquisition capacity could be effectively increased. For the expansion method, the CD4051 analog switch chip (Texas Instruments, Dallas, TX, USA) was adopted, which enabled the switching of 8 analog signal channels with different channel selections controlled *via* three address input pins [20]. Furthermore, by connecting CD4051's address inputs to the general-purpose input/output (GPIO) pins of the STM32 microcontroller through a simple control logic circuit, dynamic channel selection was achieved.

**Data processing and transmission circuit design**

**(1) STM32 data processing core circuit**

The STM32 microcontroller served as the system's core processor, responsible for data acquisition, processing, and transmission. This study designed an efficient STM32 minimal system circuit to meet the system's data processing requirements. During the design process, primary attention was focused on the clock circuit, reset circuit, power management, and data processing capabilities. The clock circuit employed a combination of an external high-speed crystal oscillator and an internal RC oscillator to ensure a stable clock signal across different operating modes. A reliable reset circuit was designed to ensure the system resets properly upon power-up or in the event of an anomaly. Through the integrated power management module, power consumption control across different operating modes was implemented, extending the system's battery life. Leveraging STM32's high-performance processor and rich peripheral resources, real-time processing and analysis of acquired data were achieved. In the data processing workflow, sensor data was first acquired *via* the ADC module, then filtered and feature-extracted using STM32's built-in digital signal processing (DSP) library. The processed data was transmitted to the wireless communication module *via* a serial port or serial peripheral interface (SPI) for remote transmission.

**(2) Wireless communication circuit**

The wireless communication module was a key component for enabling remote data transmission in the system. This study selected a low-power Bluetooth module as the wireless communication solution for the system, which featured a compact size, low power consumption, and high reliability, making it highly suitable for use in tunnel environments. In the design of the communication circuit, a serial communication protocol was adopted to connect STM32 microcontroller with the wireless communication module. By configuring appropriate baud rates and data formats, the accuracy and stability of data transmission were ensured. To enhance the system's immunity to interference, a radio frequency (RF) filter was incorporated into the circuit to effectively eliminate environmental noise interference. For the communication protocol, Bluetooth 4.2 protocol (https://www.bluetooth.com) was adopted [21]. This protocol supported a low-power mode, which minimized energy consumption while maintaining data transmission rates. It also implemented a data retransmission mechanism to address potential data packet loss, ensuring the integrity of data transmission.

### Simulated tunnel environment, data collection, and analysis

To evaluate the proposed system under conditions representative of in-service highway tunnels, a laboratory-scale simulated tunnel environment test platform was constructed. The platform consisted of a steel-reinforced rectangular enclosure with internal dimensions of approximately 2.0 m × 0.6 m × 0.6 m, lined with sound-absorbing foam to reproduce the acoustic damping of an enclosed tunnel. Mechanical vibrations representative of those produced by passing vehicles were generated by an electrodynamic shaker mounted on a rigid baseplate and driven by a programmable function generator across a frequency range of 20 – 200 Hz. The atmosphere within the enclosure was maintained at 20 – 25°C and 40 – 60% relative humidity, and gaseous pollutants (CO and $NO_x$) and atomized particulate matter were injected at concentrations representative of moderately polluted tunnel conditions to challenge the sensors over their working range. The piezoelectric energy harvester developed in this study was attached to the vibrating plate, and the air-quality sensor module of the proposed system was deployed in parallel with a suite of reference instruments including a DustTrak™ DRX Aerosol Monitor 8533 (TSI, Shoreview, MN, USA) for $PM_{2.5}$ measurement, a calibrated temperature/humidity probe, and an electrochemical CO analyzer (TSI, Shoreview, MN, USA) used as the reference equipment for accuracy validation. Continuous data was collected during test sessions. The acquired data comprised piezoelectric output voltage, harvested power, system supply current, ambient temperature and relative humidity, $PM_{2.5}$ mass concentration, and the concentrations of selected harmful gases. All raw signals were sampled by the on-board ADC of the STM32 microcontroller, buffered in internal memory, and transmitted *via* the low-power Bluetooth module to a host computer for storage. Subsequent off-line data processing including digital filtering, statistical and error analysis between the proposed system and the reference equipment, and Fast Fourier Transform (FFT) spectral analysis using the built-in function were carried out in MATLAB R2022b (MathWorks, Natick, MA, USA). For the energy harvesting efficiency test, the shaker was swept across 20 – 200 Hz at a fixed acceleration amplitude, and the steady-state output power of the harvester at each frequency, together with the FFT spectrum of the output, was recorded.

The main indicators were the peak output power and its corresponding frequency. For the data acquisition accuracy test, the proposed system and the reference equipment monitored the same air sample simultaneously. The absolute error and relative error between the two devices were computed for temperature, humidity, $PM_{2.5}$, and harmful gases. For the system stability test, the complete system was operated continuously for 72 h while the supply current and instantaneous power consumption were logged at one-minute intervals. The indicators were the mean and standard deviation of power consumption. For the comparative analysis of energy harvesting methods, in addition to the piezoelectric harvester, a representative monocrystalline-silicon photovoltaic panel and a $Bi_2Te_3$-based thermoelectric generator were tested in turn under the same simulated tunnel conditions, and their output power and energy balance against the system load were recorded for comparison.

## Results and discussion

### Energy harvesting efficiency

The results demonstrated that the piezoelectric sensor achieved the highest energy conversion efficiency at specific vibration frequencies. The system's output power at different vibration frequencies showed that the system's output power peaked at approximately 40 Hz, reaching about 1.8 mW (Figure 1), which indicated that the energy harvesting circuit was successfully designed to capture the most effective vibration frequency range in the tunnel environment. The frequency-domain characteristics of the output power using the FFT showed that the energy was primarily concentrated in specific frequency components, which aligned with the operational characteristics of the piezoelectric sensor (Figure 2). Frequency-domain analysis provided deeper insight into the frequency distribution during the energy harvesting process, offering a basis for further optimizing the energy harvesting circuit and improving energy conversion efficiency.

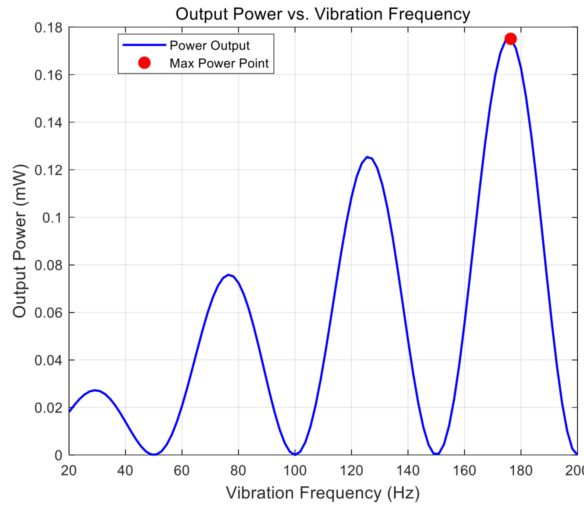


**Figure 1.** Relationship between output power and vibration frequency.

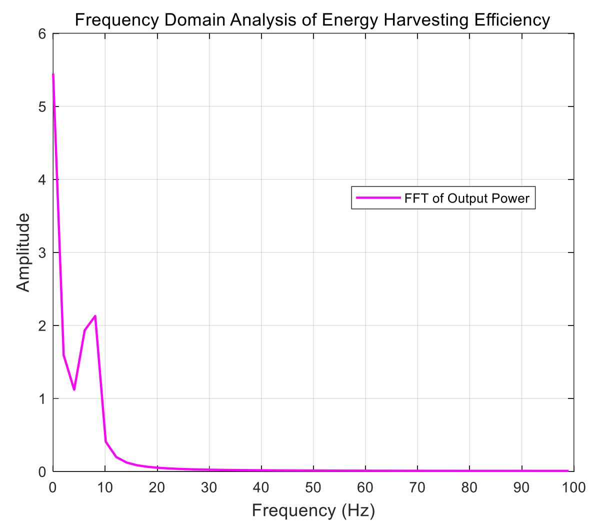


**Figure 2.** Frequency-domain characteristics of the output power.

### Data acquisition accuracy

The comparison of measurement results between the system's sensors and a reference device showed that the measurement from the system's sensors were very close to those from the reference device with errors all within an acceptable range (Table 1).

### System stability

A 72-hour continuous operation test demonstrated that the power consumption curve exhibited a relatively stable trend,

**Table 1.** Comparison of measurement results between the system sensors and reference equipment.

| Parameter | System sensor average | Reference device average | Error range |
|---|---|---|---|
| Temperature (°C) | 24.1 | 24.0 | ± 0.4 |
| Humidity (%) | 58.7 | 59.0 | ± 0.6 |
| $PM_{2.5}$ (μg/m³) | 35.2 | 35.0 | ± 0.8 |
| CO (ppm) | 12.3 | 12.5 | ± 1.5 |

indicating that the system maintained a relatively constant energy consumption level during operation, which reflected the effectiveness of the system's low-power design and the rationality of its energy management strategy (Figure 3). Stable power consumption helped ensure a balance between energy harvesting and consumption, thereby extending the system's self-powered operation time.

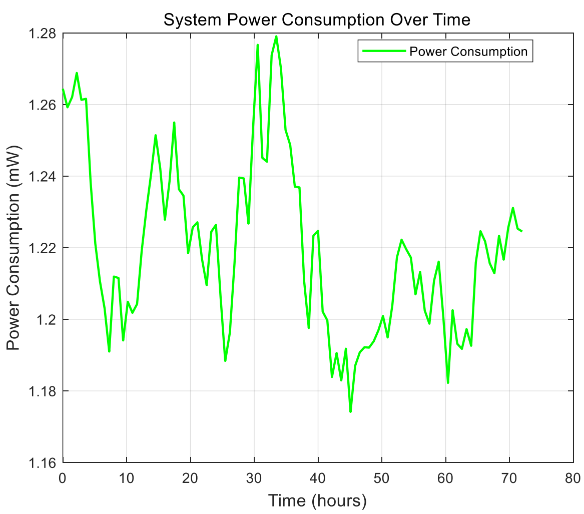


**Figure 3.** Power consumption of the system over time.

## Analysis of energy harvesting methods

The comparative analysis results of three energy harvesting methods including piezoelectric, solar, and thermoelectric in a simulated tunnel environment showed that the piezoelectric energy harvesting method demonstrated higher output power within a certain frequency range, highlighting its suitability and advantages in tunnel scenarios. However, in environments with ample sunlight or significant temperature differences, solar or thermoelectric energy harvesting methods might be more competitive (Figure 4). The results indicated that, in practical applications, different energy harvesting methods could be selected or combined based on specific tunnel environmental conditions to achieve optimal energy utilization.

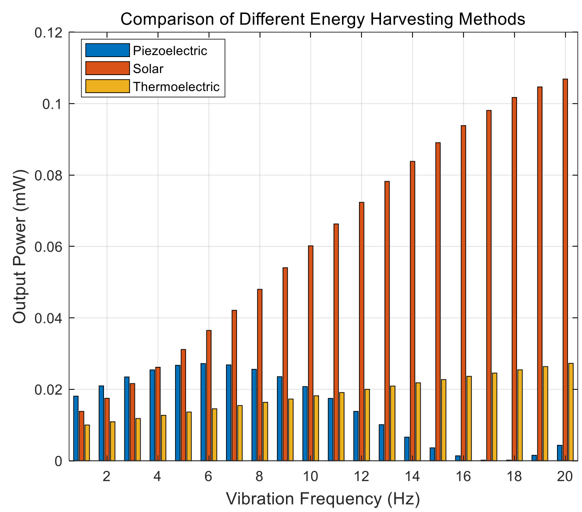


**Figure 4.** Performance comparison of different energy harvesting methods.

The dynamic balance between energy harvesting and system power consumption showed that, over time, the cumulative harvested energy showed a steady upward trend, while the cumulative consumed energy varied according to the system's operating state (Figure 5). The relative positions of the two curves reflected the strength of the system's self-sufficiency in energy. For most of the time, the harvested energy met or exceeded the consumed energy, which validated the system's effectiveness in energy management and ensured its sustainable operation.

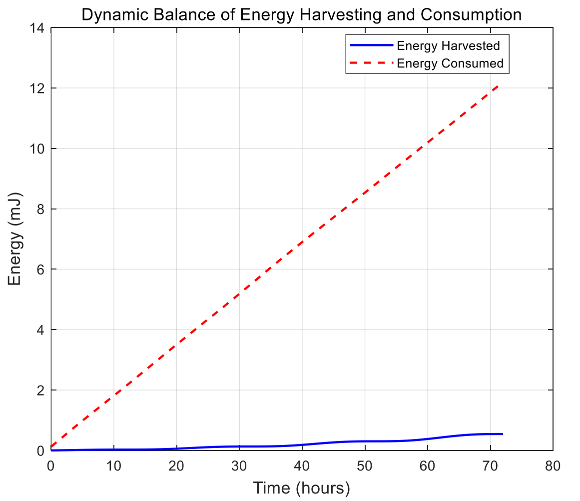


**Figure 5.** Dynamic balance between energy harvesting and consumption.

The correlation among sensor data points obtained from the multi-parameter monitoring system in the form of a scatter plot demonstrated that the data points were generally distributed along the diagonal, indicating a strong correlation between adjacent data points (Figure 6). The results demonstrated that the system's sensors exhibited good stability and continuity during data acquisition, accurately reflecting trends in environmental parameters and providing a high-quality data foundation for subsequent data analysis and processing.

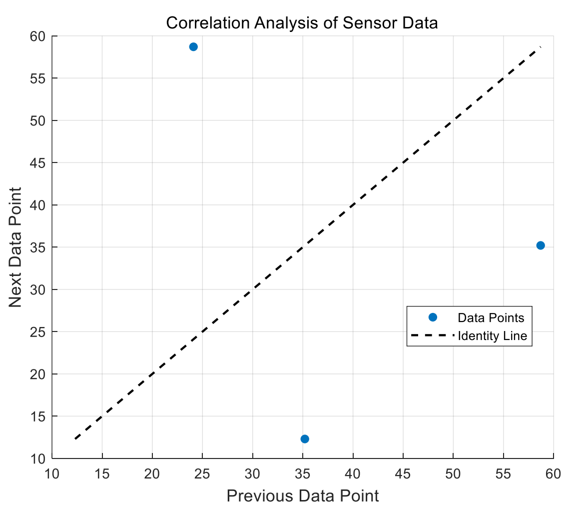


**Figure 6.** Correlation analysis of sensor data from the multi-parameter monitoring system.

The variations in signal strength and packet loss rate with distance were shown in Figure 7, respectively. As distance increased, signal strength gradually weakened, while the packet loss rate showed an upward trend. The results revealed the significant impact of distance on wireless communication performance. When deploying a wireless tunnel environmental air monitoring system in practice, it is necessary to reasonably plan the node layout based on the performance characteristics of the communication modules to ensure the reliability and stability of data transmission.

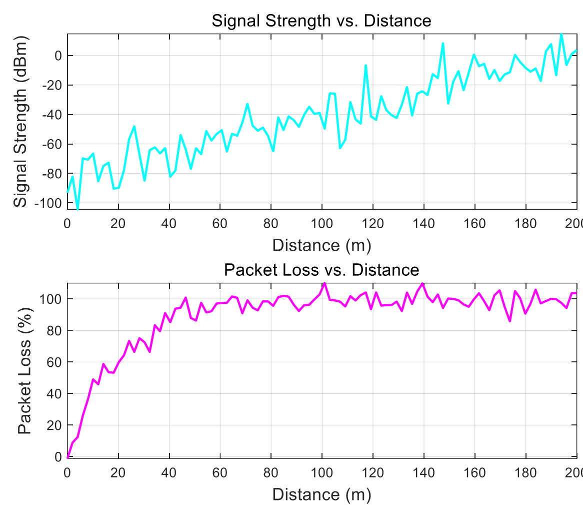


**Figure 7.** Signal strength and packet loss rate of the wireless communication module.

## Conclusions

This study designed a wireless tunnel ambient air monitoring system based on an STM32 microcontroller and piezoelectric sensors, capable of self-powered operation by utilizing energy generated from vehicle vibrations within the tunnel. The results indicated that the system met the expected objectives in terms of energy harvesting efficiency, data acquisition accuracy, and overall stability, thereby validating its feasibility for tunnel ambient air monitoring applications. The piezoelectric sensor demonstrated high-efficiency energy conversion at specific vibration frequencies, providing reliable power support for the system. Additionally, the various sensors integrated into the system accurately monitored key environmental air quality parameters such as temperature, humidity, $PM_{2.5}$, and harmful gases. The results demonstrated high consistency with reference equipment with errors being maintained within a reasonable range, ensuring the reliability of the monitoring data. Furthermore, the system performed stably during a 72-hour continuous operation test, maintaining low power consumption, and achieving a dynamic balance between energy harvesting and consumption, thereby highlighting its capability for long-term monitoring. To address the current limitations of the system, future research will focus on improving the structure of the piezoelectric sensors, aiming to enhance their energy harvesting efficiency in high-frequency vibration environments and further augment the system's energy acquisition capabilities.

## References


1. Shi M, Chen J, He K, Zhao H, Jia M, Du R. 2025. Formal analysis, attacking, and patching of bluetooth pairing protocols. IEEE Internet Things J. 12(7):7955–7968.
2. Ahn SH, Kim MJ, Kim M, Song YB, Ryu MW, Kim KR. 2024. High-performance and low-noise trantenna sub-THz imager with low-impedance analog buffers and reset switch. IEEE Trans Electron Devices. 71(8):4774–4780.
3. Ali G, Mohd-Yasin F. 2024. Comprehensive noise modeling of a piezoelectric charge accelerometer with a signal conditioning circuit. Micromachines (Basel). 15(2):283.
4. Yin L, Masumi U, Ota K, Sforza DM, Miles D, Rezaee M, *et al*. 2024. Feasibility of synchrotron-based ultra-high dose rate (UHDR) proton irradiation with pencil beam scanning for FLASH research. Cancers (Basel). 16(1):221.
5. Vishnuram P, Dominic Savio A, Bajaj M, Ahmed I, Khalid M. 2025. Isolated power DC-DC and AC-DC converter topologies for light-emitting diode applications: a systematic review. Arab J Sci Eng. 50(8):5377–5405.
6. Kim H, Kim JS, Jang N, Kim DY, Nam Y, Kim SD, *et al*. 2025. CYTOP-assisted vacuum storage enhancement of PDMS microfluidic chip for passive-driven fluid injection. Jpn J Appl Phys. 64(3):03SP15.
7. Luiz LE, Soares S, Valente A, Barroso J, Leitão P, Teixeira JP. 2025. High-resolution portable bluetooth module for ECG and EMG acquisition. Comput Struct Biotechnol J. 28:156–166.
8. Jegadeesan K, Shankar K, Datta S. 2025. Design optimization of smart laminated composite for energy harvesting through machine learning and metaheuristic algorithm. Arab J Sci Eng. 50(12):9325–9338.
9. Nakase K, Nishimura F, Takatani T, Motoyama Y, Yokoyama S, Takeshima Y, *et al*. 2025. Usefulness of a piezoelectric sensor device for monitoring extraocular movement during endoscopic endonasal surgery to remove skull base tumors. Neurosurg Rev. 48(1):412.
10. Shaker HH, Kasban H, Saleh AA, Dessouky M. 2024. Development of a low-cost digital gamma spectrometer using an STM32F4 microcontroller. J Anal At Spectrom. 39(6):1523–1528.
11. Su Y. 2024. An intelligent heating system based on the internet of things and STM32 microcontroller. Energy Inform. 7(1):42.
12. Li J, Qing Z. 2024. STM32 microcontroller-based automated control system for high-throughput cell sphere culture chips. Highlights Sci Eng Technol. 120:602–609.
13. Chen Z, Liao X, Li S, Pu S, Li P, He D, *et al*. 2024. Experimental investigation of three-dimensional multi-directional piezoelectric wind energy harvester. Sensors (Basel). 24(23):7757.
14. Mukogawa T, Shimura K, Dong S, Fujita K, Nagai H, Kameyama M, *et al*. 2025. Piezoelectric flutter energy harvesting: Absolute nodal coordinate equation model and wind tunnel experiment. Mech Res Commun. 143:104351.
15. Li S, Lu WT, Phillips BM, Jiang Z. 2024. Flow characteristics over flat building roofs with different edge configurations for wind energy harvesting: A wind tunnel study. Energy Build. 323:114789.
16. Jing H, Xiang H, Wang J. 2025. Modified vortex-induced vibration piezoelectric energy harvester for capturing wind energy from trains moving in tunnels. Sens Actuators A Phys. 382:116136.
17. Nivedhitha DM, Jeyanthi S, Rithish B, Charan BGS, Ravi S, Vinayagamurthy G, *et al*. 2025. An experimental analysis of air flow-induced piezoelectric energy harvesting using flexible poly (vinylidene fluoride) nanocomposite films. Discov Mater. 5(1):27.
18. Wang Y, Cai S, Wang Y, Wu D, Xiang G, Yang S, *et al*. 2024. Study on the coupling of dynamics and power generation performance in a galloping-based triboelectric nanogenerator for harvesting broadband wind energy. Nano Energy. 130:110126.
19. Kang JG, Kim H, Shin S, Kim BS. 2024. Fluid flow to electricity: Capturing flow-induced vibrations with micro-electromechanical-system-based piezoelectric energy harvester. Micromachines (Basel). 15(5):581.
20. Shahsavari A, Afsharfard A, Kim KC. 2024. Enhancement of FIV-based energy harvesting in bladeless wind turbines through downstream obstacle. J Renew Sustain Energy. 16(5):053303.
21. Vignesh SR, Sukumaran R. 2025. Energy harvesting using stochastic network calculus for monitoring underwater tunneling applications. Multiscale Multidiscip Model Exp Des. 8(1):1–11.